



# Hemodynamic Analysis of Endoleaks After Endovascular Abdominal Aortic Aneurysm Repair by Using 4-Dimensional Flow-Sensitive Magnetic Resonance Imaging

Mayu Sakata, MD; Yasuo Takehara, MD, PhD; Kazuto Katahashi, MD; Masaki Sano, MD, PhD; Kazunori Inuzuka, MD, PhD; Naoto Yamamoto, MD; Masataka Sugiyama, MD; Harumi Sakahara, MD, PhD; Tetsuya Wakayama, PhD; Marcus T. Alley, PhD; Hiroyuki Konno, MD, PhD; Naoki Unno, MD, PhD

**Background:** An endoleak is a common complication of endovascular abdominal aortic aneurysm repair (EVAR), and it can be associated with aneurysmal growth. This pilot study used 4-dimensional flow-sensitive magnetic resonance imaging (4D-flow) to assess the hemodynamics of different types of endoleaks (I–IV).

**Methods and Results:** Magnetic resonance angiography, 4D-flow, and computed tomography angiography (CTA) were performed in 31 patients after nitinol-based stent-graft deployment. With 4D-flow, the 3D streamlines of endoleaks appear as integrated traces along the instantaneous velocity vector field that are color-coded according to the local velocity magnitude of the leak. The 4D-flow analysis identified endoleaks in 18 patients (58.1%), whereas CTA identified endoleaks in 13 patients (41.9%). The 4D-flow analysis created a characteristic image of each type of endoleak. Among patients with endoleaks, 4D-flow identified concomitant multiple endoleaks in 7 (39%) patients, and it further differentiated type II endoleaks from type IIa endoleaks (to-and-fro biphasic flow pattern from a branch vessel) and from type IIb endoleaks (monophasic flow pattern with a connection between the inflow and outflow branches).

**Conclusions:** The 4D-flow analysis was more sensitive than CTA for detecting an endoleak, and it could subclassify type II endoleaks. In addition, 4D-flow differentiated between concomitant endoleak types in a single patient. (*Circ J* 2016; **80**: 1715–1725)

**Key Words:** 4D-flow; Endoleaks; Hemodynamics; Magnetic resonance imaging; Stent-graft

Endovascular aortic aneurysm repair (EVAR) is widely performed because it is a safe and minimally invasive technique.<sup>1,2</sup> However, it is associated with reintervention in approximately 30% of cases during long-term follow-up.<sup>3,4</sup> An endoleak is defined as persistent blood flow within the aneurysmal sac but outside the stent-graft.<sup>5</sup> Among the types of endoleaks, a type II endoleak reportedly accounts for >50% of all post-EVAR reinterventions.<sup>6</sup> When an endoleak causes enlargement of the aneurysmal sac, additional treatments such as transarterial embolization, translumbar embolization, or open repair can prevent sac rupture.<sup>7,8</sup> However, not all endoleaks are associated with sac enlargement. Currently, there are 5 known types of endoleaks according to the leakage pattern, and the management of an endoleak is type-specific.<sup>8</sup>

During EVAR follow-up, computed tomography angiography (CTA) surveillance is commonly performed to detect endoleaks. However, it can be difficult to classify an endoleak on the basis of CTA findings alone, especially because multiple types of endoleaks can occur concomitantly, and in such cases, it is difficult to discern which endoleak is the dominant one. Furthermore, it is impossible to determine the most significant endoleak in terms of the patient's prognosis.

Compared with CTA, magnetic resonance angiography (MRA) is more sensitive for detecting an endoleak after EVAR with nitinol-based devices.<sup>9–13</sup> Furthermore, dynamic contrast-enhanced magnetic resonance imaging (MRI)-based angiography may offer the additional advantage of classifying endoleaks.<sup>14</sup> Recently, time-resolved phase contrast MRI with

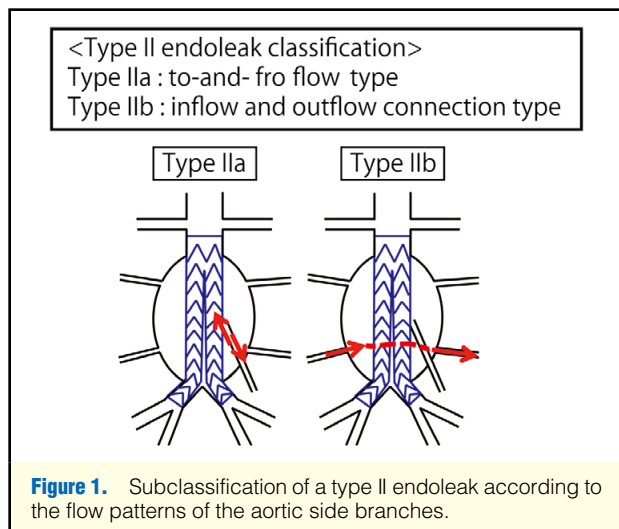
Received March 29, 2016; revised manuscript received May 15, 2016; accepted May 16, 2016; released online June 29, 2016 Time for primary review: 9 days

Second Department of Surgery (M. Sakata, K.K., M. Sano, K.I., N.Y., H.K., N.U.), Department of Radiology (Y.T., M. Sugiyama, H.S.), Hamamatsu University School of Medicine, Hamamatsu; GE Healthcare Japan, Hino (T.W.), Japan; and Department of Radiology, Stanford University, Palo Alto, CA (M.T.A.), USA

Mailing address: Naoki Unno, MD, PhD, Second Department of Surgery, Hamamatsu University School of Medicine, 1-20-1 Handayama, Higashi-ku, Hamamatsu 431-3192, Japan. E-mail: unno@hama-med.ac.jp

ISSN-1346-9843 doi:10.1253/circj.CJ-16-0297

All rights are reserved to the Japanese Circulation Society. For permissions, please e-mail: [cj@j-circ.or.jp](mailto:cj@j-circ.or.jp)



velocity encoding along the flow directions and 3-dimensional (D) anatomic coverage (4D-flow) has emerged as a novel technique that enables the comprehensive evaluation of complex blood flow and flexible, retrospective quantification of the flow parameters.<sup>15–17</sup> The purpose of the present study was to use 4D-flow to better understand post-EVAR endoleak subtype patterns.

## Methods

This study was approved by the Institutional Review Board of the University School of Medicine, Hamamatsu, Japan. Written informed consent for publication of the report and any accompanying images was given by the patients who were enrolled in this study.

### Study Population

Between January 1, 2013 and August 31, 2014, 73 patients with an infrarenal abdominal aortic aneurysm (AAA) underwent elective operation. Among them, open repair of the AAA was performed in 7 patients, and EVAR was performed in 66; 53 (80%) patients received nitinol-based stent-grafts (34 received the Endurant stent-graft [Medtronic, Minneapolis, MN, USA] and 19 received the Excluder stent-graft [Gore Medical, Flagstaff, AZ, USA]). Of those, 31 patients with normal renal function or a slight renal function disorder (estimated glomerular filtration rate  $>30$  ml/min/1.73 m<sup>2</sup>) were enrolled. CTA, MRA, duplex ultrasonography and 4D-flow were performed within 60 days postoperatively. The mean time interval between MRA and CTA was 5.6 days (range, 0–45 days). Interpretations of the CTA, MRA, and 4D-flow findings were performed in a blinded manner for comparison, and at least 2 physicians independently read the images of each modality and compared the results.

### Contrast-Enhanced Computed Tomography (CT)

Contrast-enhanced CT was also performed for all patients, using a multidetector-row CT Aquilion 64 scanner (Toshiba Medical Systems, Tochigi, Japan) or SOMATOM Definition Flash scanner (Siemens Medical Systems, Erlangen, Germany). The typical field of view (FOV) (cm) was 40×43, pitch factor was 0.8 with a rotation speed of 0.3–0.5 s and the matrix was 512×512. We used 350–370 mgI/ml of iodinated contrast media (Iopamiron 370, Bayer Healthcare, Osaka, Japan; Omnipaque 350, Daiichi

Sankyo Co, Tokyo, Japan; or Iomeron 350, Bracco Eisai, Milan, Italy). In each case, 2 ml/kg body weight of contrast medium was injected at a rate of 4 ml/s followed by a chaser bolus of 20 ml of saline solution using an autoinjector (Dual Shot GX, Nemoto Kyorindo, Tokyo). The pre-phrase and 3 phases of post-contrast acquisitions were made after the contrast injection was initiated.

### Time-Resolved Contrast-Enhanced 3D MRA

All patients underwent a magnetic resonance (MR) examination using a 3.0 Tesla MR scanner (Discovery MR 750 and 32-channel torso array coil, GE Healthcare, Waukesha, WI, USA).

Prior to 4D-flow analysis, contrast-enhanced 3D MRA was performed after a bolus injection of gadolinium chelate at a standard dosage of 0.1 mmol/kg and an injection rate of 2–3 ml/s was administered with an autoinjector. The contrast agent was used to increase the definition of the arterial wall boundary for post-processing and increase the signal-to-noise ratio of the 4D-flow measurement. A coronal 3D fast spoiled gradient echo sequence was used with the following parameters: repetition time (TR) (ms)/echo time (TE) (ms)/flip angle (FA) (degree)/number of excitations (NEX), 2.6/0.8/15/1; FOV, 34–48×33.6 cm; partition thickness, 2 mm; slice zero fill interpolation, 2; overlaps, 2 mm; matrix, 224×224; receiver bandwidth, 83.3 kHz; array spatial sensitivity encoding technique reduction factor, 2; 60 partitions ×6; and scan time, 35s. The best arterial phase 3D data set was selected from the 6 phases, and it was used for segmenting the boundary of the aortic wall or stent-graft by the maximum intensity projection algorithm.

### Assessment Using 4D-Flow Analysis

The 4D-flow analysis was performed by covering the abdominal aorta, inferior mesenteric artery (IMA), and lumbar arteries (LAs) using a retrospective ECG-gated technique. It was conducted with the following parameters: TR (ms)/TE (ms)/FA (degree)/NEX, 4.5–5.0/1.6–2.0/15/1; FOV, 34–48 cm; matrix, 224–256×160–224; partition thickness, 1–2 mm; 40–60 partitions; 12 phases; approximate imaging time, 5–7 min; and reduction factor, 2 for an autocalibrating reconstruction for Cartesian sampling. The encoding velocity was determined on the basis of the maximum flow velocity value measured with 2D phase contrast cine MRI, to which a safety margin of 10 cm/s was added.

### Post-Processing of the 4D-Flow Data

The 4D-flow and MRA data sets were transferred to a personal computer (Intel Core™ i7 CPU, 3.2 GHz, 12 GB RAM, Microsoft Windows 7; Microsoft Corp, Redmond, WA, USA) in Digital Imaging and Communications in Medicine format, and they were post-processed using flow analysis software (Flova, Renaissance Technology, Hamamatsu, Japan). The application consisted of 2 processes of extraction and analysis. First, time-resolved images of the 3D velocity vector fields were generated to overview the blood flow within the abdominal aorta. Next, 3D streamlines were generated from the 4D data sets.

### Generation of Endoleak 3D Streamlines

The 3D streamlines are integrated traces along the instantaneous velocity vector field that are color-coded according to the local velocity magnitude of the leak. When analyzing type II endoleaks, sectional planes were selected at the vertical section of branch vessels of the aneurysmal sac, such as the IMA and LAs. To analyze type I and III endoleaks, sectional planes were

**Table.** Hemodynamic Analysis of 4D-Flow in All Patients Undergoing Repair of Abdominal Aortic Aneurysm

Patient no.	Initial AAA diameter (mm)	Stent-graft	Detection and classification of endoleak by intraoperative completion angiography (DSA)	Detection of endoleak by CTA	Detection of endoleak by Duplex ultrasonography	Type of endoleak on 4D-flow
1	49	Endurant	–	–	–	Ila
2	44	Endurant	IV	+	+	Ila
3	55	Endurant	–	–	–	–
4	88	Endurant	IV	–	–	Ila
5	57	Endurant	II	–	–	–
6	57	Endurant	IV	+	–	II+IV
7	55	Endurant	IV	+	+	II+III
8	52	Endurant	II	–	–	–
9	52	Endurant	IV	+	+	II+IV
10	50	Endurant	I	+	–	I+II+III
11	55	Excluder	III	+	–	I+II+III
12	52	Endurant	–	–	–	II+III
13	48	Endurant	–	+	–	Ila
14	49	Excluder	–	+	+	Ilb
15	50	Endurant	IV	–	–	IV
16	57	Excluder	–	+	+	Ila
17	50	Excluder	–	–	–	–
18	48	Endurant	IV	+	+	II+III
19	53	Endurant	–	–	–	–
20	60	Endurant	IV	–	–	Ila
21	50	Excluder	–	–	–	–
22	50	Endurant	–	–	–	–
23	74	Excluder	–	+	–	Ilb
24	52	Endurant	–	–	–	–
25	61	Endurant	–	–	–	–
26	52	Excluder	–	–	–	–
27	55	Endurant	–	–	–	–
28	55	Excluder	II	+	–	Ila
29	50	Endurant	–	–	–	–
30	51	Excluder	II	+	–	Ilb
31	52	Endurant	–	–	–	–

+, Positive detection of endoleak on CTA; –, negative detection of endoleak. AAA, abdominal aortic aneurysm; CTA, computed tomography angiography; D, dimensional; DSA, digital subtraction angiography.

selected at the vertical sections just below the proximal edge of the stent-graft, and just below the leg joint of the stent-graft, respectively. Several cross-sectional planes of the abdominal aorta, IMA, and LAs were selected for analysis. All planes were placed perpendicular to the longitudinal axis of the artery. Streamlines were generated by the Runge-Kutta method.<sup>16</sup>

### Subclassification of a Type II Endoleak

Hemodynamic analysis with 4D-flow demonstrated that a type II endoleak can be further classified into 2 distinct subtypes according to the flow patterns of the aortic side branches (Figure 1). Examples of the typical imaging features of each subclassification of a type II endoleak are described below. When concomitant endoleaks with multiple types were identified (ie, type I+II+III, II+III, or II+IV), we did not subclassify type II endoleaks into type Ila and Ilb, because the flow tracing would be difficult and confusing.

**Type Ila Endoleak** Type Ila endoleaks were to-and-fro biphasic flow leaks in which LAs and/or the IMA show peri-

odical changes in the blood flow direction from retrograde to antegrade.

**Type Ilb Endoleak** Type Ilb endoleaks are inflow-and-outflow connection-type leaks in which there is a connection between the inflow and outflow aortic branches (ie, the IMA or LAs). The 4D-flow analysis shows a vessel perfusing the aortic sac (inflow in a retrograde manner) that connects with another vessel of the aortic sac (outflow in an antegrade manner).

### Identification of a Concomitant Endoleak

In the 4D-flow analysis, each flow can be traced, so clinicians can determine where the flow originates and whether the flow connects to other vessels of the AAA sac. For example, if there is a type Ia endoleak and the flow connects to a LA, it is categorized as a type Ia. However, if there is a type Ia endoleak and a to-and-fro type II endoleak that does not connect to a type Ia flow (ie, it comes from a solitary vessel), then it is categorized as a type I+II. Whenever the endoleak is a type II, there should be at least 1 inflow vessel from outside of the sac.

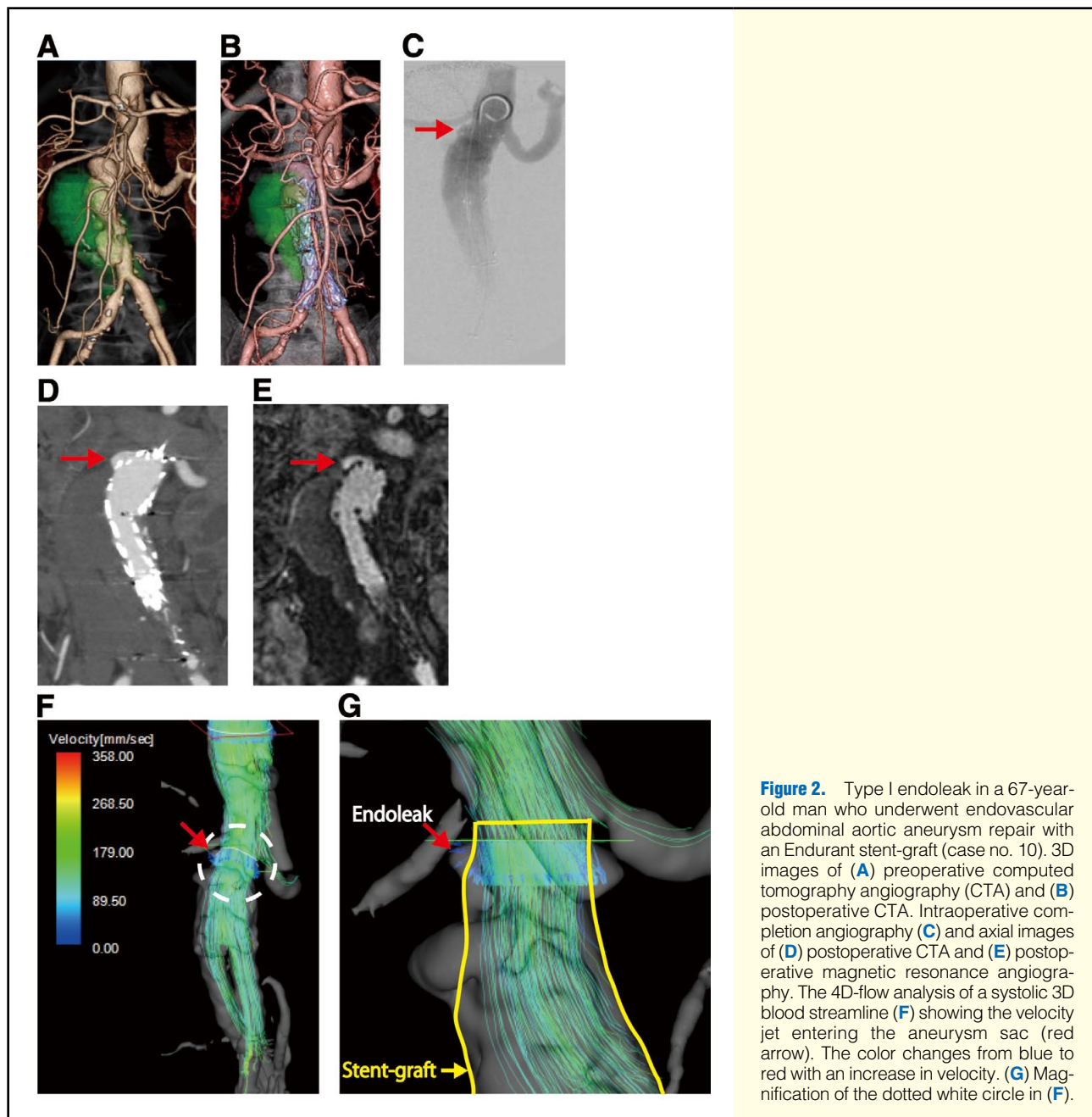


**Figure 2.** Type I endoleak in a 67-year-old man who underwent endovascular abdominal aortic aneurysm repair with an Endurant stent-graft (case no. 10). 3D images of (A) preoperative computed tomography angiography (CTA) and (B) postoperative CTA. Intraoperative completion angiography (C) and axial images of (D) postoperative CTA and (E) postoperative magnetic resonance angiography. The 4D-flow analysis of a systolic 3D blood streamline (F) showing the velocity jet entering the aneurysm sac (red arrow). The color changes from blue to red with an increase in velocity. (G) Magnification of the dotted white circle in (F).

## Results

### Hemodynamic Analysis of Each Type of Endoleak

Results of the hemodynamic analysis of 4D-flow in all patients are shown in the [Table](#). The 4D-flow analysis identified endoleaks in 18 of 31 (58.1%) patients, CTA identified endoleaks in 13 patients (41.9%), and duplex ultrasonography identified endoleaks in 6 patients (19.4%). When the sensitivity and specificity of intraoperative completion arteriography were both 1.0, the sensitivity and specificity were 0.85 and 0.65 for 4D-flow, 0.64 and 0.76 for CTA, and 0.29 and 0.88 for duplex ultrasonography, respectively. Among the 18 cases, 111 branch vessels of the sac were identified, and hemodynamics of the blood flow were analyzed. Endoleaks were classified according to their subtype (I–IV). According to 4D-flow, type I, II, III, or IV

endoleak frequencies were 6.5%, 54.8%, 16.1%, and 9.7%, respectively. Among the 18 cases with an endoleak, 4D-flow analysis demonstrated 7 cases (39%) of concomitant multiple types of endoleaks. Examples of the typical imaging features of each type are described below.

### Type I Endoleak

**Figure 2** shows a type I endoleak in a 67-year-old man who underwent EVAR with an Endurant stent-graft (case 10, [Figures 2A,B](#)). Intraoperative completion angiography showed a type Ia endoleak ([Figure 2C](#)) below the proximal portion of the stent-graft. Postoperative CTA and MRA clearly showed a type Ia endoleak ([Figures 2D,E](#)). 4D-flow analysis of the type Ia endoleak showed the jet flow of the velocity streamlines entering the aneurysmal sac at the proximal neck ([Figures 2F,G](#);

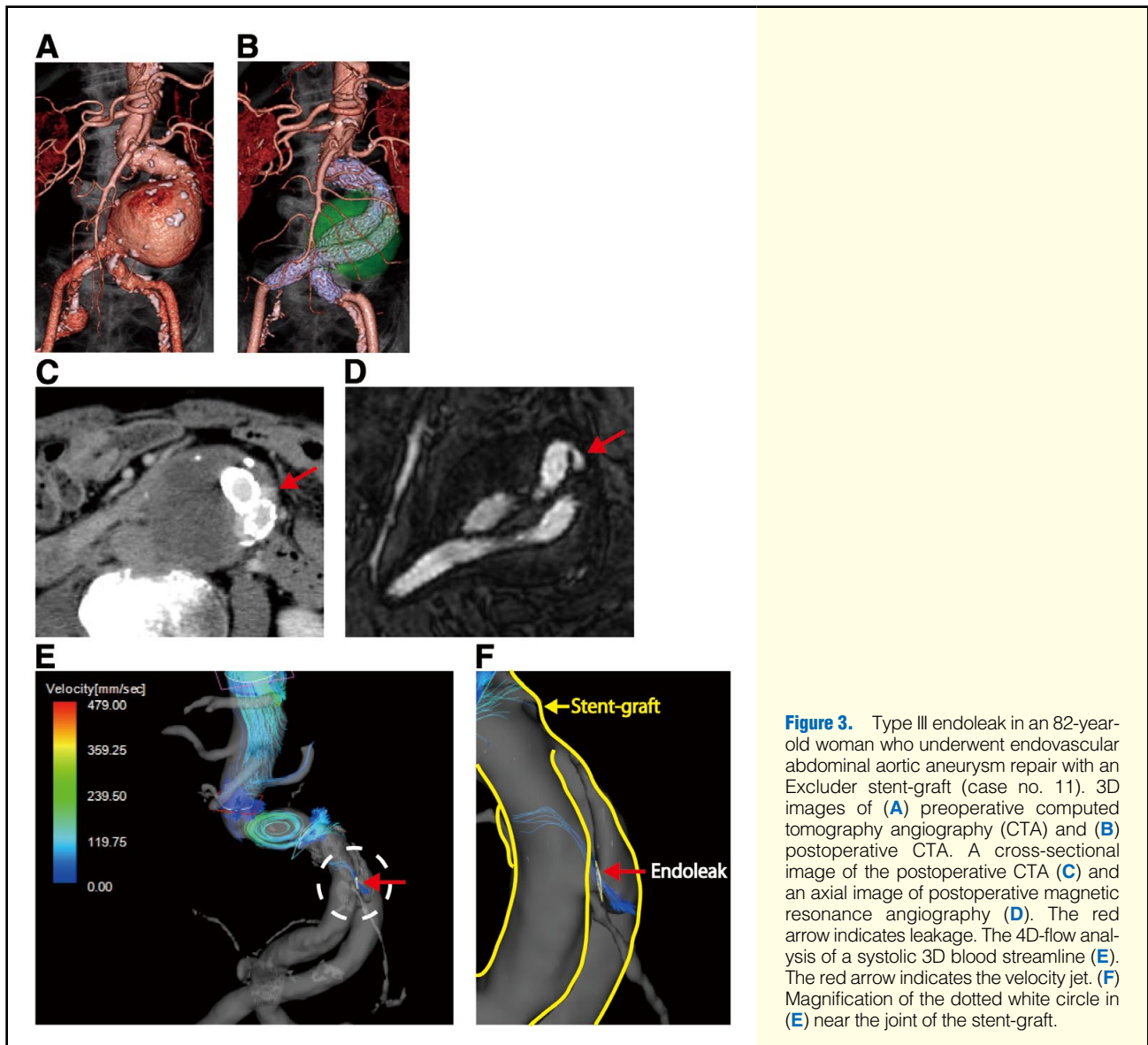


**Figure 3.** Type III endoleak in an 82-year-old woman who underwent endovascular abdominal aortic aneurysm repair with an Excluder stent-graft (case no. 11). 3D images of (A) preoperative computed tomography angiography (CTA) and (B) postoperative CTA. A cross-sectional image of the postoperative CTA (C) and an axial image of postoperative magnetic resonance angiography (D). The red arrow indicates leakage. The 4D-flow analysis of a systolic 3D blood streamline (E). The red arrow indicates the velocity jet. (F) Magnification of the dotted white circle in (E) near the joint of the stent-graft.

#### Movie S1).

#### Type III Endoleak

**Figure 3** shows a type III endoleak in an 82-year-old woman who underwent EVAR with an Excluder stent-graft (case 11, **Figures 3A,B**). Intraoperative completion angiography detected an endoleak, and postoperative CTA and MRA showed contrast leakage near the contralateral limb (left side) of the stent-graft. There is a joint between the contra-gate and the leg of the stent-graft (**Figures 3C,D**). The 4D-flow analysis showed the jet flow of the velocity streamline from the leg to the aneurysmal sac, confirming a type III endoleak (**Figures 3E,F**; **Movie S1**). The endoleak may have occurred because of the severe angulation of the proximal neck. The patient was followed at the outpatient clinic.

#### Type IV Endoleak

**Figure 4** shows a type IV endoleak in an 83-year-old man who underwent EVAR with an Endurant stent-graft (case 6, **Figures 4A,B**). MRA on postoperative day 1 clearly showed

diffuse leakage of contrast medium around the stent-graft (**Figures 4C,D**). The early and late phases of 4D-flow showed that the jet flow velocity streamlines entered the aneurysmal sac from the stent-graft, and extended in all directions (**Figures 4E,F**; **Movie S1**).

#### Type II endoleak

**Type IIa Endoleak** **Figure 5** shows a typical case of a type IIa endoleak in a 72-year-old man who underwent EVAR with an Endurant stent-graft (case 13, **Figure 5A**). Preoperative CTA and MRA showed good patency of the IMA (**Figures 5B,D**). Postoperative CTA and MRA demonstrated a type II endoleak from the IMA (**Figures 5C,E**), which was the only vessel perfusing the inside of the aortic sac. The 4D-flow analysis identified that the blood flow direction in the IMA changed periodically from retrograde to antegrade (to-and-fro) (**Figure 5F**; **Movie S2**).

**Type IIb Endoleak** **Figure 6** shows a typical case of a type IIb endoleak in a 74-year-old man who underwent EVAR with an Excluder stent-graft (case 23, **Figure 6A**). A comparison

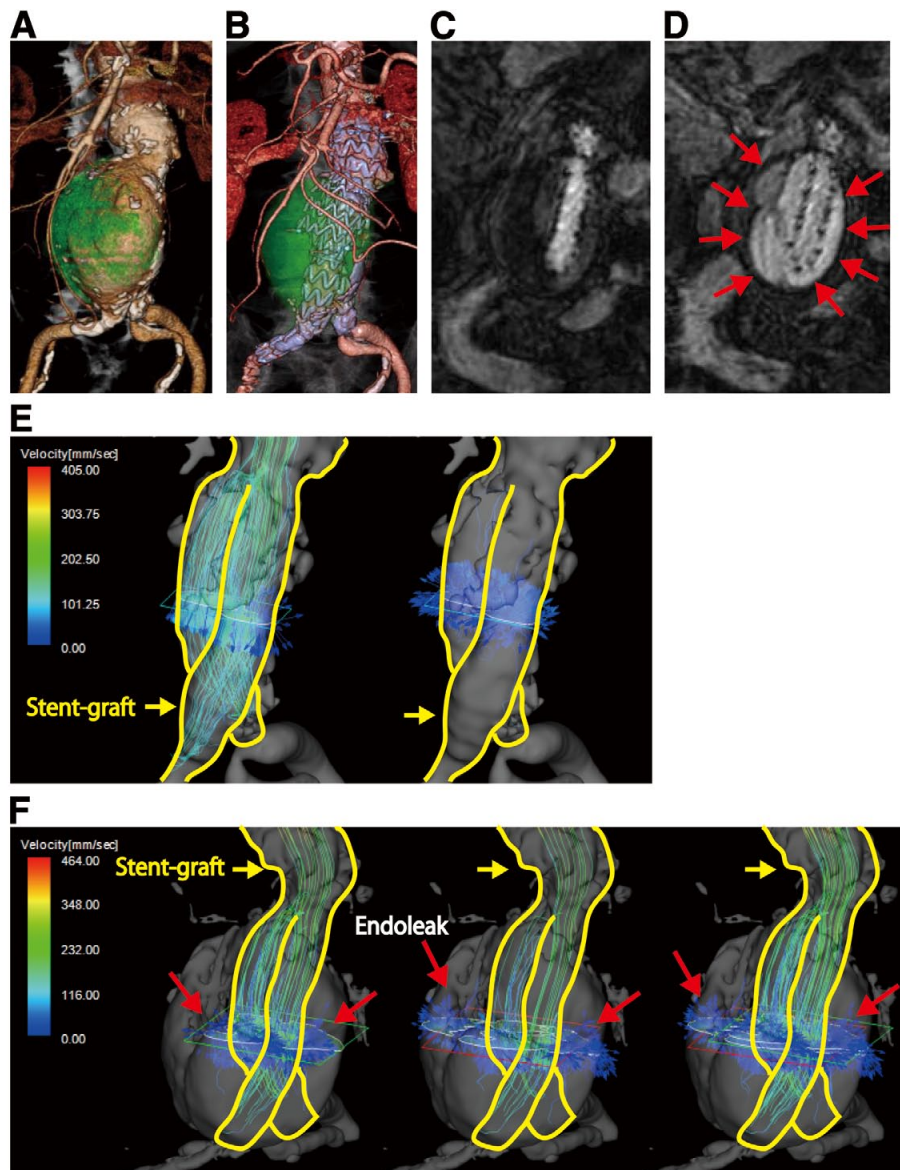


**Figure 4.** Type IV endoleak in an 83-year-old man who underwent endovascular abdominal aortic aneurysm repair with an Endurant stent-graft (case no. 6). 3D images of preoperative computed tomography angiography (CTA) (A) and postoperative CTA (B). Dynamic magnetic resonance angiography on postoperative day 1 (C,D). The red arrows indicate leakage of the contrast medium. The 4D-flow analysis of a systolic 3D blood streamline (E,F) showing the velocity jet at the early phase (E) and late phase (F) entering the aneurysm sac and extending in all directions.

of the pre- and post-EVAR CTA and MRA identified a contrast leakage near the 4th right LA (R4) and the 4th left LA (L4) (Figures 6B–E). The 4D-flow analysis confirmed the connection between the inflow and outflow branches, which is characteristic of a type IIb endoleak (Figure 6F; Movie S3).

### Discussion

We demonstrated the use of 4D-flow analysis for evaluating the hemodynamics of endoleaks after nitinol-based stent-graft deployment. By using this novel technique, an endoleak was evaluated according to the conventional classification (types I–IV). The assessment of 31 patients after EVAR by 4D-flow

analysis showed that this technique was more sensitive and informative for assessing endoleaks than CTA.

CTA is commonly used for post-EVAR surveillance because of its rapid acquisition time and high diagnostic value. However, the superiority of MRA for detecting an endoleak has been previously reported.<sup>11,13,14</sup> A previous study reported that CTA detected post-EVAR endoleaks in 20–40% of patients, whereas the detection rate for MRA was 70–80%.<sup>12</sup> In particular, MRA was superior to CTA for detecting type II endoleaks. Typically, triphasic, unenhanced, arterial, and delayed phase CTA is performed for post-EVAR surveillance; however, it often fails to detect the type II endoleaks detected by MRA.<sup>12,18</sup> In our study, intraoperative completion angiography identified

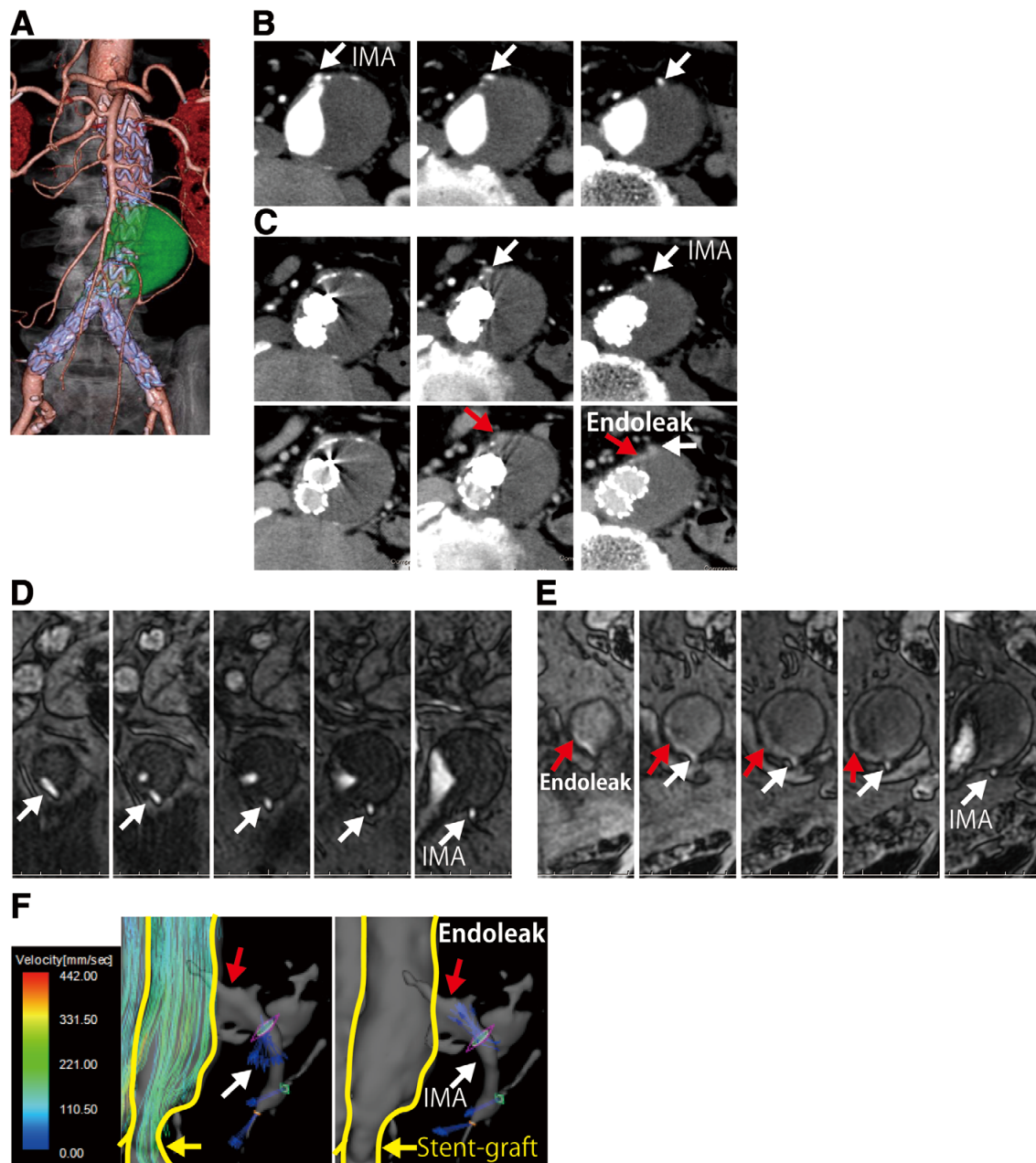


**Figure 5.** Type IIa endoleak in a 72-year-old man who underwent endovascular abdominal aortic aneurysm repair with an Endurant stent-graft (case no. 13). 3D postoperative computed tomography angiography (CTA) (A). Cross-sectional images of preoperative CTA (B), postoperative CTA (C), and a patent IMA (D). Cross-sectional images of the postoperative magnetic resonance angiography (E) and 4D-flow analysis of a systolic 3D blood streamline (F). IMA, inferior mesenteric artery.

endoleaks >50% of the time at the end of surgery (Table). However, the use of an Endurant stent-graft is often accompanied with a type IV endoleak in Asian countries, because smaller diameter devices are deployed for the smaller aorta in Asian patients compared with Western patients. Although a type IV endoleak usually disappears within 10 days, the occurrence of a leakage can mask the presence of other types of endoleaks such as types II and III. We identified types II and/or III endoleaks in case nos. 2, 4, 6, 7, 9, 18, and 20 on MRA, but these types may have been masked by type IV endoleaks on intra-

operative completion angiography. Because MRA has a high sensitivity, intrinsic 3-dimensionality and better soft tissue contrast, it should be considered in patients with a growing aneurysm, even if an endoleak is not detected on CT surveillance. Indeed, we experienced a case of a patient who had post-EVAR sac expansion without signs of an endoleak on CTA but positive signs of an endoleak on MRA (Figures 7A–D). The 4D-flow analysis identified the origin of the endoleak via the median sacral artery (Figure 7E). On the other hand, 4D-flow analysis may be associated with higher false-positives in

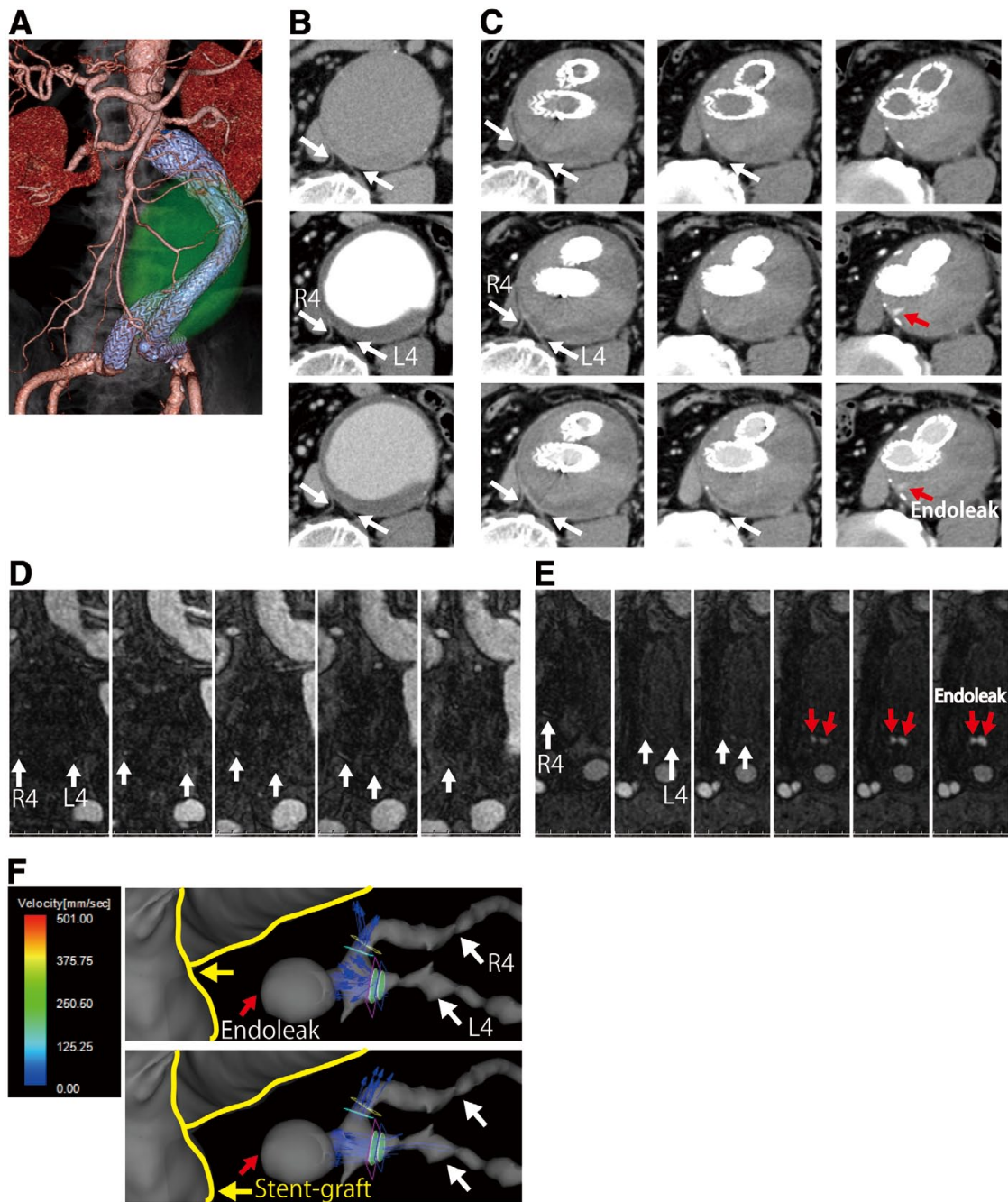


**Figure 6.** Type IIb endoleak in a 74-year-old man who underwent endovascular abdominal aortic aneurysm repair with an Excluder stent-graft (case no. 23). 3D postoperative computed tomography angiography (CTA) (A). Cross-sectional images of preoperative CTA (B) and postoperative CTA (C). Axial images of the postoperative magnetic resonance angiography (D). The white arrows indicate contrast medium in the aneurysmal sac from the 4th right lumbar artery (R4) to the 4th left lumbar artery (L4). R4 and L4 had a connection inside the sac (red arrows) (E). The 4D-flow analysis of a systolic 3D blood streamline (F) showing the connection between L4 and R4.

endoleak detection. In case nos. 1 and 12, which the endoleak was not detected by CT/ultrasound but by 4D-flow, the maximum diameter of the AAA sac showed no change in case no.1 and a decrease in case no. 12 at 1 year after EVAR. The follow-up results suggested that endoleaks detected only by 4D-flow might be either false-positive or clinically insignificant to

expand the AAA sac hemodynamically. Therefore, 4D-flow may be utilized not for post-EVAR monitoring/screening for endoleaks but as the secondary modality after CT/duplex ultrasound for selecting patients who need reintervention.

The 4D character of acquisition (3-spatial and one temporal dimension) does provide additional hemodynamic information

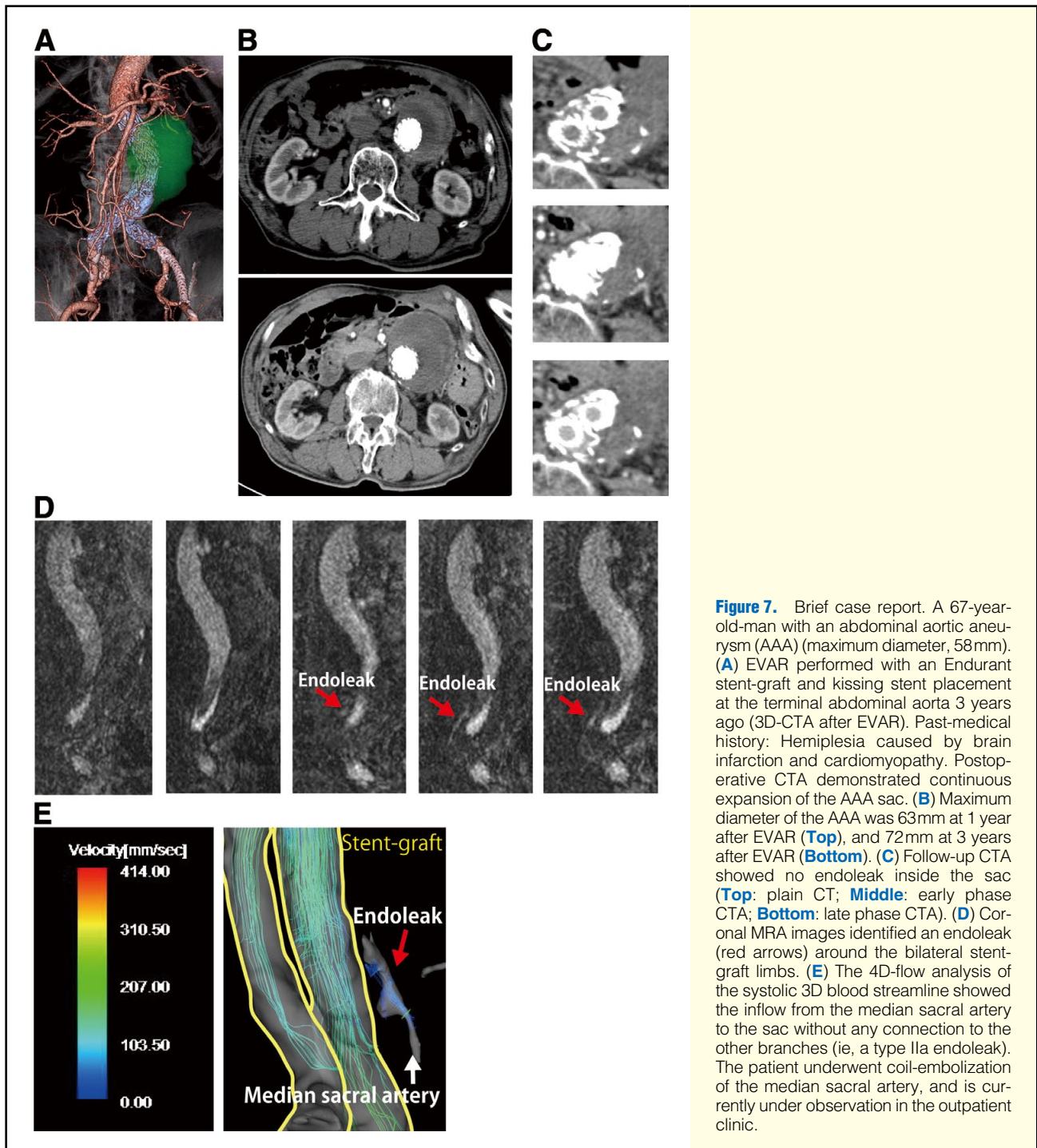


**Figure 7.** Brief case report. A 67-year-old-man with an abdominal aortic aneurysm (AAA) (maximum diameter, 58mm). **(A)** EVAR performed with an Endurant stent-graft and kissing stent placement at the terminal abdominal aorta 3 years ago (3D-CTA after EVAR). Past-medical history: Hemiparesis caused by brain infarction and cardiomyopathy. Postoperative CTA demonstrated continuous expansion of the AAA sac. **(B)** Maximum diameter of the AAA was 63mm at 1 year after EVAR (**Top**), and 72mm at 3 years after EVAR (**Bottom**). **(C)** Follow-up CTA showed no endoleak inside the sac (**Top**: plain CT; **Middle**: early phase CTA; **Bottom**: late phase CTA). **(D)** Coronal MRA images identified an endoleak (red arrows) around the bilateral stent-graft limbs. **(E)** The 4D-flow analysis of the systolic 3D blood streamline showed the inflow from the median sacral artery to the sac without any connection to the other branches (ie, a type IIa endoleak). The patient underwent coil-embolization of the median sacral artery, and is currently under observation in the outpatient clinic.

about the endoleak.<sup>19</sup> Several studies have demonstrated the usefulness of 4D-flow in hemodynamic assessments of the heart, thoracic aorta, abdominal aorta, branch vessels of the abdominal aorta, and intracranial vasculature.<sup>15,16,20–23</sup> Regarding endoleak analysis, Hope et al previously studied type I endoleaks by 4D-flow;<sup>24</sup> however, other types of endoleaks have not been investigated, possibly because it is difficult to assess the aortic side branches with 4D-flow.

In the present study, we successfully analyzed all types of endoleaks by 4D-flow, and, by evaluating the hemodynamics of each side branch, type II endoleaks were further classified

into types IIa and IIb. Considering that an endoleak was detected in nearly 50% of patients after EVAR, clinicians should assume that a type II endoleak may be a manifestation of collateral flows into the aneurysmal sac (ie, an endoleak may be an intrinsic occurrence because of the basic principle of EVAR, which was often not detectable by the available means until now). With 4D-flow, it was also possible to differentiate between concomitant endoleaks in each case. For example, when proximal type Ia endoleaks, type II endoleaks between the IMA and LAs, and type III endoleaks at the leg joint of the stent-graft occur simultaneously, only 4D-flow enables each endoleak

to be classified by analyzing the blood flow streamlines and tracing. Considering that the presence of an endoleak is associated with lower aneurysm regression and is the cause of AAA rupture in up to 70% of all cases,<sup>25</sup> any improvement in the endoleak surveillance methods is paramount for an improved clinical benefit. According to CTA surveillance, a type II endoleak occurs with the highest frequency in 20–30% of all EVAR cases. The severity of a type II endoleak has received renewed interest;<sup>26–28</sup> among post-EVAR AAA rupture cases, 10–20% of patients had a type II endoleak, and the mortality rate of a post-EVAR AAA rupture is approximately 50%.<sup>25,29</sup> However, predicting patients with a type II endoleak who are at risk of aneurysm growth is challenging, and management of this type of endoleak remains controversial. Some authors have advocated a conservative approach to all type II endoleaks.<sup>30</sup> Others have supported a more aggressive approach with intervention in all cases,<sup>31</sup> or they have even proposed preoperative embolization of aortic side branches to prevent a type II endoleak.<sup>32,33</sup> Insufficient information concerning each subclass of type II endoleaks most likely accounts for the diverse management tactics for type II endoleaks. The 4D-flow analysis showed the flow pattern (ie, the flow direction and phase shift) and measured the blood flow volume and velocity of each endoleak-associated branch vessel. There are clearly 2 patterns of blood flow in type II-associated vessels. Previously, a type II endoleak was characterized as either a simple type (2a) with 1 patent collateral branch or a complex type (2b) with  $\geq 2$  collateral branches.<sup>34</sup> However, our classification of a type II endoleak is different, because we classified the responsible vessels of an endoleak on the basis of the flow direction. The 4D-flow analysis can provide vector images of blood flow in each vessel, which enables clinicians to distinguish blood vessels with to-and-fro blood flow toward the sac (type IIa) from that with continuous one-way blood flow (type IIb). A type IIb endoleak indicates that at least 1 pair of endoleak vessels with inflow and outflow is present. Long-term follow-up with 4D-flow analysis may help clinicians determine the best management for endoleaks and choose which endoleak vessels require a second intervention to prevent aneurysmal rupture. Considering that a persistent type II endoleak is associated with secondary interventions and aneurysm rupture, determining a type II endoleak consistently would help clinicians determine the best management strategy for endoleaks. Long-term follow-up with 4D-flow analysis has been continued in post-EVAR patients, which may address these questions in the near future.

### Study Limitations

First, the sample size was small. Second, the analysis of 4D-flow depended on spatial and temporal resolution at 2 mm<sup>3</sup> and 40 ms, respectively. Therefore, smaller aortic side branches that connect with the leaking branch artery may go undetected, which can lead to a misdiagnosis in cases of type IIb. In addition, 4D-flow could not be used with stainless-based stent-grafts. It is also difficult to use MRA/4D-flow analysis with a gadolinium contrast agent in patients with chronic kidney disease (estimated glomerular filtration rate  $<30$  ml/min/1.73 m<sup>2</sup>) or those on dialysis, because there is an increased risk of the potential occurrence of nephrogenic systemic fibrosis.

### Conclusions

We performed MRA and 4D-flow analysis in the initial phase of post-EVAR surveillance. MRA was more sensitive for detecting type II endoleaks than CTA. The 4D-flow analysis

demonstrated that most endoleaks consisted of concomitant multiple types, and it further differentiated a type II endoleak as types IIa and IIb, according to the hemodynamics of each aortic side branch blood flow. MRA analysis with 4D-flow in post-EVAR patients can provide more hemodynamic information about endoleaks. Further studies with an accumulation of long-term follow-up data may enable clinicians to predict the outcome of endoleaks and aneurysms.

### Funding Sources

This work was supported by JSPS KAKENHI grant no. 26293310 and 16K15629 (N.U.), JSPS KAKENHI grant no. 26462103 (N.Y.), and JSPS KAKENHI grant no. 00397415 (K.I.) from the Japan Science and Technology Agency.

### Competing Interests

M.T.A. received research grants from GE Healthcare. T.W. is an employee of GE Healthcare Japan, which is the vendor of the MR system used in this study. The remaining authors declare no conflicts of interest.

### Authors' Contributions

Conceived and designed the experiments (study design): N.U. Recruited and registered patients (data collection): K.K., M. Sano, K.I., N.Y., and M. Sugiyama. Analyzed and interpreted the data (data analysis): M. Sakata, Y.T., K.K., N.U., T.W., H.S., H.K., Y.T., and M.T.A. Contributed to the materials/analysis tools: M.T.A., T.W., M. Sugiyama, H.S., and H.K. Revised the manuscript critically for important intellectual content: Y.T., M.T.A., M. Sugiyama, H.S., H.K., and N.U. Wrote the manuscript (writing): M. Sakata, Y.T., and N.U.

### References

1. JCS Joint Working Group. Guidelines for diagnosis and treatment of aortic aneurysm and aortic dissection (JCS 2011): Digest version. *Circ J* 2013; **77**: 789–828.
2. Yamamoto K, Komori K, Banno H, Narita H, Kodama A, Sugimoto M. Validation of patient selection for endovascular aneurysm repair or open repair of abdominal aortic aneurysm: Single-center study. *Circ J* 2015; **79**: 1699–1705.
3. De Bruin JL, Baas AF, Buth J, Prinssen M, Verhoeven EL, Cuypers PW, et al. Long-term outcome of open or endovascular repair of abdominal aortic aneurysm. *N Engl J Med* 2010; **362**: 1881–1889.
4. Greenhalgh RM, Brown LC, Powell JT, Thompson SG, Epstein D, Sculpher MJ. Endovascular versus open repair of abdominal aortic aneurysm. *N Engl J Med* 2010; **362**: 1863–1871.
5. White GH, Yu W, May J, Chaufour X, Stephen MS. Endoleak as a complication of endoluminal grafting of abdominal aortic aneurysms: Classification, incidence, diagnosis, and management. *J Endovasc Surg* 1997; **4**: 152–168.
6. EVAR trial participants. Endovascular aneurysm repair versus open repair in patients with abdominal aortic aneurysm (EVAR trial 1): Randomised controlled trial. *Lancet* 2005; **365**: 2179–2186.
7. Baum RA, Carpenter JP, Golden MA, Velazquez OC, Clark TW, Stavropoulos SW, et al. Treatment of type 2 endoleaks after endovascular repair of abdominal aortic aneurysms: Comparison of transarterial and translumbar techniques. *J Vasc Surg* 2002; **35**: 23–29.
8. Moll FL, Powell JT, Fraedrich G, Verzini F, Haulon S, Waltham M, et al. Management of abdominal aortic aneurysms clinical practice guidelines of the European society for vascular surgery. *Eur J Vasc Endovasc Surg* 2011; **41**(Suppl 1): S1–S58.
9. van der Laan MJ, Bartels LW, Viergever MA, Blankensteijn JD. Computed tomography versus magnetic resonance imaging of endoleaks after EVAR. *Eur J Vasc Endovasc Surg* 2006; **32**: 361–365.
10. Saba L, Montisci R, Sanfilippo R, Mallarini G. Imaging of the endoleak after endovascular aneurysm repair procedure by using multidetector computer tomography angiography. *J Cardiovasc Surg* 2009; **50**: 515–526.
11. Wieners G, Meyer F, Halloul Z, Peters N, Ruhl R, Dudeck O, et al. Detection of type II endoleak after endovascular aortic repair: Comparison between magnetic resonance angiography and blood-pool contrast agent and dual-phase computed tomography angiography. *Cardiovasc Intervent Radiol* 2010; **33**: 1135–1142.
12. Ichihashi S, Marugami N, Tanaka T, Iwakoshi S, Kurumatani N, Kitano S, et al. Preliminary experience with superparamagnetic iron oxide-enhanced dynamic magnetic resonance imaging and comparison

- with contrast-enhanced computed tomography in endoleak detection after endovascular aneurysm repair. *J Vasc Surg* 2013; **58**: 66–72.
13. Habets J, Zandvoort HJ, Reitsma JB, Bartels LW, Moll FL, Leiner T, et al. Magnetic resonance imaging is more sensitive than computed tomography angiography for the detection of endoleaks after endovascular abdominal aortic aneurysm repair: A systematic review. *Eur J Vasc Endovasc Surg* 2013; **45**: 340–350.
  14. van der Laan MJ, Bakker CJ, Blankensteijn JD, Bartels LW. Dynamic CE-MRA for endoleak classification after endovascular aneurysm repair. *Eur J Vasc Endovasc Surg* 2006; **31**: 130–135.
  15. Mano Y, Takehara Y, Sakaguchi T, Alley MT, Isoda H, Shimizu T, et al. Hemodynamic assessment of celiaco-mesenteric anastomosis in patients with pancreaticoduodenal artery aneurysm concomitant with celiac artery occlusion using flow-sensitive four-dimensional magnetic resonance imaging. *Eur J Vasc Endovasc Surg* 2013; **46**: 321–328.
  16. Stankovic Z, Allen BD, Garcia J, Jarvis KB, Markl M. 4D flow imaging with MRI. *Cardiovasc Diagn Ther* 2014; **4**: 173–192.
  17. Suwa K, Saitoh T, Takehara Y, Sano M, Nobuhara M, Saotome M, et al. Characteristics of intra-left atrial flow dynamics and factors affecting formation of the vortex flow analysis with phase-resolved 3-dimensional cine phase contrast magnetic resonance imaging. *Circ J* 2015; **79**: 144–152.
  18. Haulon S, Lions C, McFadden EP, Koussa M, Gaxotte V, Halna P, et al. Prospective evaluation of magnetic resonance imaging after endovascular treatment of infrarenal aortic aneurysms. *Eur J Vasc Endovasc Surg* 2001; **22**: 62–69.
  19. Markl M, Chan FP, Alley MT, Wedding KL, Draney MT, Elkins CJ, et al. Time-resolved three-dimensional phase-contrast MRI. *J Magn Reson Imaging* 2003; **17**: 499–506.
  20. Wetzel S, Meckel S, Frydrychowicz A, Bonati L, Radue EW, Scheffler K, et al. In vivo assessment and visualization of intracranial arterial hemodynamics with flow-sensitized 4D MR imaging at 3T. *Am J Neuroradiol* 2007; **28**: 433–438.
  21. Markl M, Kilner PJ, Ebberts T. Comprehensive 4D velocity mapping of the heart and great vessels by cardiovascular magnetic resonance. *J Cardiovasc Magn Reson* 2011; **13**: 7.
  22. Hsiao A, Lustig M, Alley MT, Murphy MJ, Vasanaawala SS. Evaluation of valvular insufficiency and shunts with parallel-imaging compressed-sensing 4D phase-contrast MR imaging with stereoscopic 3D velocity-fusion volume-rendered visualization. *Radiology* 2012; **265**: 87–95.
  23. Barker AJ, Markl M, Burk J, Lorenz R, Bock J, Bauer S, et al. Bicuspid aortic valve is associated with altered wall shear stress in the ascending aorta. *Circ Cardiovasc Imaging* 2012; **5**: 457–466.
  24. Hope TA, Zarins CK, Herfkens RJ. Initial experience characterizing a type I endoleak from velocity profiles using time-resolved three-dimensional phase-contrast MRI. *J Vasc Surg* 2009; **49**: 1580–1584.
  25. Schlosser FJ, Gusberg RJ, Dardik A, Lin PH, Verhagen HJ, Moll FL, et al. Aneurysm rupture after EVAR: Can the ultimate failure be predicted? *Eur J Vasc Endovasc Surg* 2009; **37**: 15–22.
  26. Harris PL, Vallabhaneni SR, Desgranges P, Becquemin JP, van Marrewijk C, Laheij RJ. Incidence and risk factors of late rupture, conversion, and death after endovascular repair of infrarenal aortic aneurysms: The EUROSTAR experience: European Collaborators on Stent/graft techniques for aortic aneurysm repair. *J Vasc Surg* 2000; **32**: 739–749.
  27. Timaran CH, Ohki T, Veith FJ, Lipsitz EC, Gargiulo NJ 3rd, Rhee SJ, et al. Influence of type II endoleak volume on aneurysm wall pressure and distribution in an experimental model. *J Vasc Surg* 2005; **41**: 657–663.
  28. El Batti S, Cochenec F, Roudot-Thoraval F, Becquemin JP. Type II endoleaks after endovascular repair of abdominal aortic aneurysm are not always a benign condition. *J Vasc Surg* 2013; **57**: 1291–1297.
  29. Mehta M, Paty PS, Roddy SP, Taggart JB, Sternbach Y, Kreinberg PB, et al. Treatment options for delayed AAA rupture following endovascular repair. *J Vasc Surg* 2011; **53**: 14–20.
  30. Rayt HS, Sandford RM, Salem M, Bown MJ, London NJ, Sayers RD. Conservative management of type 2 endoleaks is not associated with increased risk of aneurysm rupture. *Eur J Vasc Endovasc Surg* 2009; **38**: 718–723.
  31. Solis MM, Ayerdi J, Babcock GA, Parra JR, McLafferty RB, Gruneiro LA, et al. Mechanism of failure in the treatment of type II endoleak with percutaneous coil embolization. *J Vasc Surg* 2002; **36**: 485–491.
  32. Sheehan MK, Hagino RT, Canby E, Wholey MH, Postoak D, Suri R, et al. Type 2 endoleaks after abdominal aortic aneurysm stent grafting with systematic mesenteric and lumbar coil embolization. *Ann Vasc Surg* 2006; **20**: 458–463.
  33. Ward TJ, Cohen S, Fischman AM, Kim E, Nowakowski FS, Ellozy SH, et al. Preoperative inferior mesenteric artery embolization before endovascular aneurysm repair: Decreased incidence of type II endoleak and aneurysm sac enlargement with 24-month follow-up. *J Vasc Interv Radiol* 2013; **24**: 49–55.
  34. Shah A, Stavropoulos SW. Treatment strategies for type 2 endoleaks after endovascular aneurysm repair. *Acta Chir Belg* 2007; **107**: 356–360.

### Supplementary Files

#### Supplementary File 1

**Movie S1.** 3D visualization of the blood streamline of a type I endoleak in case no. 10, a type III endoleak in case no. 11, and a type IV endoleak in case no. 6.

#### Supplementary File 2

**Movie S2.** 3D visualization of the blood streamline of type IIa endoleak in case no. 13.

#### Supplementary File 3

**Movie S3.** 3D visualization of the blood streamline of type IIb endoleak in case no. 23.

Please find supplementary file(s);  
<http://dx.doi.org/10.1253/circj.CJ-16-0297>